

Optimal Placement of Distributed Generation Units for Microgrid Planning in Distribution Networks

Shah Mohammad Rezwanul Haque Shawon, *Student Member, IEEE*, Xiaodong Liang , *Senior Member, IEEE*, and Mehrnoosh Janbakhsh, *Senior Member, IEEE*

Abstract—Due to increasing penetration of renewable distributed generation (DG), conventional distribution networks have been gradually transforming into their active form, where microgrids may serve as fundamental building blocks. As the primary step towards microgrid planning, optimal DGs placement and sizing can reduce the total energy losses by localizing power supply to loads. In this paper, a DG optimal placement method by minimizing the total energy losses is proposed, where the planning is formulated as a non-linear programming (NLP) problem. AC optimal power flow (OPF) is used to solve this planning problem by considering operational constraints and uncertainties in load and renewable power generation of the network. IEEE 33-bus test system and a real 404-bus distribution system operated by Saskatoon Light and Power in Saskatoon, Canada are used to validate the proposed method. The proposed method also shows superior performance compared to existing methods.

Index Terms—AC optimal power flow, distributed generation, microgrid planning, non-linear programming, optimal placement, uncertainty modeling.

I. INTRODUCTION

WITH continuous increase in global energy demand, renewable energy sources are enablers for tomorrow's sustainable power grids. The degree of utilization of renewables in today's energy market can be seen through simple statistics. As per the World Wind Energy Association (WWEA), with the addition of 93 GW wind power capacity in 2020, the total wind power generation capacity worldwide reached 744 GW, which could supply 7% of the world's energy demand. According to International Renewable Energy Agency (IRENA), the total

solar photovoltaic (PV) installed capacity worldwide in 2020 is 709 GW.

Increasing penetration of renewable distributed generation (DG) in distribution networks brings environmental benefits, as well as challenges for planning study due to uncertainties associated with renewables. Implementation of microgrids in distribution networks is an effective way to integrate both conventional and renewable DG units and minimize energy losses by localizing power generation and load consumption [1], [2]. A microgrid is defined in IEEE Std. 2030.7-2017 as “a group of interconnected loads and distributed energy resources with clearly defined electrical boundaries that acts as a single controllable entity with respect to the grid and can connect and disconnect from the grid to enable it to operate in both grid-connected or island modes”. As per IEEE Std. 1547.4-2011 [3], [4], a microgrid, as the fundamental building block of active distribution systems, can reduce power losses, and improve voltage profile and reliability.

Recognizing advantages of microgrids by planners, operators and investors, microgrid planning and implementation in distribution systems have attracted significant research interests. Long power lines to distribution areas are mainly responsible for increased energy losses, and thus, optimal allocation and sizing of DGs facilitates locally supplying power to loads, and reduces energy losses [5], [6]. Improper allocation of DGs may cause operational issues in the system, such as voltage swells.

Among optimal DG placement methods, *metaheuristics* (such as evolutionary algorithms and simulated annealing), *mathematical programming* (such as linear programming (LP), mixed integer linear programming (MILP), non-linear programming (NLP), and mixed integer non-linear programming (MINLP)), and *metaheuristic search techniques* (such as Tabu search optimization and group search optimization) are popular for solving optimization problems.

For the planning problem, commonly used power flow study methods include the backward forward sweep load flow [7], probabilistic load flow [6], DistFlow equations [8], Sequential Quadratic Programming (SQP) to solve the optimal power flow (OPF) [9], and AC optimal power flow (OPF) [10]. The AC OPF approach has the ability to model operational characteristics of the network, which ensures that all operational constraints are satisfied during a planning study.

In [11], the planning problem is formulated as a MINLP to define the microgrid topology and find optimal locations and sizes of DGs, energy storage systems, and AC-DC converters to

Manuscript received 19 November 2022; accepted 7 January 2023. Date of publication 12 January 2023; date of current version 19 May 2023. Paper 2022-PSEC-1394, presented at the 2022 IEEE Industry Applications Society Annual Meeting, Detroit, MI, USA, Oct. 09–14, and approved for publication in the IEEE TRANSACTIONS ON INDUSTRY APPLICATIONS by the Power Systems Engineering Committee of the IEEE Industry Applications Society [DOI: 10.1109/IAS54023.2022.9939755]. This work was supported by the Natural Science and Engineering Research Council of Canada Discovery under Grant RGPIN-2016-04170. (Corresponding author: Xiaodong Liang.)

Shah Mohammad Rezwanul Haque Shawon and Xiaodong Liang are with the Department of Electrical and Computer Engineering, University of Saskatchewan, Saskatoon, SK S7N 5A9, Canada (e-mail: shs054@mail.usask.ca; xil659@mail.usask.ca).

Mehrnoosh Janbakhsh was with the Saskatoon Light and Power in Saskatoon, Saskatoon, SK S7N 5A9, Canada. She is now with the Distribution Engineering, BC Hydro, Burnaby, BC V3N 4X8, Canada (e-mail: mehrnoosh.janbakhsh@bchydro.com).

Color versions of one or more figures in this article are available at <https://doi.org/10.1109/TIA.2023.3236363>.

Digital Object Identifier 10.1109/TIA.2023.3236363

ensure reliable power flow with the minimum deployment and operational costs. A similar study is conducted in [12] using a deterministic branch-and-bound nonlinear solver for optimization. The method proposed in [13] simultaneously determines sizes, locations and types of DGs and shunt capacitor banks by solving the MINLP problem. An MINLP problem for the profit maximization in [14] is solved by Grey Wolf Optimization algorithm for simultaneously determining the optimal size, site, type, and number of DGs, energy storage system (ESS) and distributed reactive source (DRS). The overall planning costs including unit commitment and switching costs associated with dispatchable units are minimized in [15] by forming a nonlinear convex programming problem to obtain optimal sizes of distributed energy resources.

In [16], Genetic Algorithm (GA) is utilized in planning for siting and sizing of DGs and placement of switches, utility profits are considered by decreasing outage costs and improving customer's satisfaction in terms of reliability. Particle Swarm Optimization (PSO) and GA-based optimization techniques are used in [5] to find optimal sites and sizes of renewable energy sources for autonomous operation. The investment master problem of a planning study minimizes investment costs in [17] including microgrid operation and unserved energy costs to determine the optimal generation mix. Improved PSO is used to determine optimal number, locations, sizes and mix of DGs and capacitor banks to maximize the net profit in [18]. Minimizing the mismatch power in island mode is considered as the main objective to determine optimal sizes and locations of DGs in [19]. Optimal allocation of DGs including sizing, siting, and the optimal order of joining in the test system is proposed in [20] using Craziness-based PSO algorithm to reduce power supply costs including buying costs, power losses, communication and load shedding costs.

Teaching Learning Based Optimization (TLBO) is used to solve the optimization problem in [21] that jointly optimizes capacities and locations of dispatchable and non-dispatchable DGs and ESS. A Column and Constraint Generation (CCG) method is used to solve the two-stage robust optimization problem in [8], [22], where costs and profits are optimized in [22] to determine optimal locations, sizes and mix of DGs; while minimizing the system damage is considered as the objective of DGs allocation in [8]. Optimal size, number, and site of DG, ESS, and DRS are determined in [23] by Cuckoo Optimization Algorithm (COA) and Imperialist Competitive Algorithm (ICA). A combinatorial optimization technique is proposed in [10] to solve the optimal sizing problem by utilizing a meta-heuristic technique based on a tailor-made GA for hybrid AC–DC microgrids. Decision theory-based approaches are used in [9] to obtain the best sizing and siting solutions considering reduction of energy costs while providing ancillary services to the network. The Simulated Annealing (SA) approach is investigated in [24] to determine optimal sizes and locations of a mix of DGs at a minimum cost subject to reliability targets. The Group Search Optimization (GSO) algorithm are utilized in [6] for optimal DG placement considering the improvement of the system load factor and decreasing losses. Different types of DGs are optimally allocated for annual energy loss minimization while maintaining

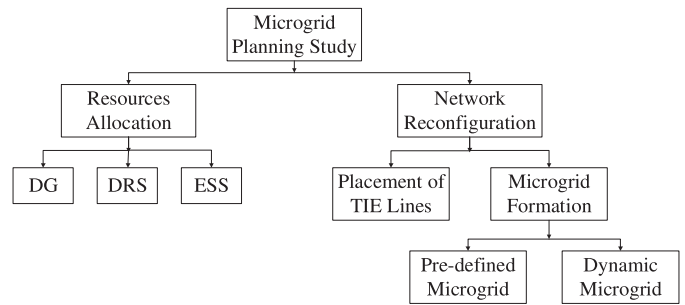


Fig. 1. Research streams of microgrid planning.

the voltage profile within acceptable limits by using Tabu Search Optimization algorithm in [25], [26], [27].

Although metaheuristic techniques are commonly used in microgrid planning study, they don't guarantee the global solution all the time, which may lead to improper allocation of DGs. Mathematical programming formulation is therefore used in this study to place DGs optimally by minimizing the total annual energy losses and improving the voltage profile of the distribution network.

The microgrid planning study in the literature can be divided into two streams [23] as shown in Fig. 1: 1) optimal allocation of resources such as DG, DRS, and ESS; and 2) reconfiguration of network by placing TIE lines and optimal microgrid formation. Optimal placement and sizing of DGs is one fundamental task in microgrid planning [15], [28].

Different factors and indices have been used to select candidate locations for DG placement in the literature. The losses-voltage-factor (LVF) is used in [21] that ensures reduced losses, the improved voltage profile, and a higher reliability. The loss sensitivity factor (LSF) and the voltage sensitivity factor (VSF) are used in [2] to determine optimal locations of DGs by reducing the system loss and improving the voltage profile, respectively. The total voltage deviation (VD) and voltage sensitivity index (VSI) are used in [29] for DG placement. Candidate buses can also be selected based on regional conditions and utility decisions [6]. All these factors to place DGs have been calculated with the voltage profile of a base network at the beginning of a planning study without considering the change in voltage levels due to the load growth, which is a common phenomenon of a distribution system. Therefore, DG locations selected based on these factors might become improper with the changed voltage levels.

To address this challenge, it is important to consider the change in the voltage profile during the planning period. A new index named "Voltage Regulation Index (VRI)" is defined in this paper by considering the change in the bus voltage profile due to the load growth during a planning period. The main contributions of the paper include:

- 1) The planning problem is formulated as a non-linear programming (NLP) for optimal DG placement by minimizing the total energy losses and improving the voltage profile of distribution networks;
- 2) Candidate locations for DG placement are selected by defining a new index, VRI, considering the change in the

bus voltage level due to the load growth during a planning period;

- 3) A non-linear AC OPF model is formulated to perform the power flow analysis by considering operational constraints of the network (such as the voltage limit, branch current limit, DG integration limit, load variation, and uncertainties of DGs);
- 4) The performance of four commercially available PV modules are analyzed using historical solar data over one year to calculate their capacity factors (CFs), and the PV module with the highest CF is selected in the planning study; and
- 5) The proposed method is validated using IEEE 33-bus test system and a real large three-phase unbalanced 404-bus distribution system operated by Saskatoon Light and Power, a Canadian electric utility in Saskatoon, Canada.

The paper is arranged as follows: the proposed optimal DG placement methodology is introduced in Section II; modeling of load, DGs and their uncertainties are conducted in Section III; the mathematical problem formulation is presented in Section IV; the proposed method is validated using IEEE 33-bus system and a real distribution system from Saskatoon Light and Power in Sections V and VI, respectively; and conclusions are drawn in Section VII.

II. THE PROPOSED METHODOLOGY FOR DG PLACEMENT

In this paper, an optimal DG placement methodology for microgrid planning in distribution networks is proposed through a NLP problem formulation and AC OPF to address operational constraints. The proposed methodology is shown in Fig. 2.

The following are four major steps of the proposed method for optimal placement of DGs:

A. Modeling of Load and DGs Considering Uncertainties

Load and renewable DGs vary stochastically. In this planning study, uncertainties associated with load and renewable power generation are modeled with a probability analysis by analyzing historical load and solar data over one year. The normal and beta distribution are used to model uncertainties of load and PV power generation, respectively. The details are discussed in Section III.

B. Selection of Candidate Buses for DG Placement

The load usually increases over time in a distribution network due to new customers, which eventually changes the bus voltage profile of the network. A new index for DG placement, VRI, is defined in (1) to account for the change in bus voltages due to load growth during a planning period.

$$\text{Voltage Regulation Index (VRI)} = \frac{V_{i_{base}} - V_{i_{after}}}{V_{i_{after}}} \quad (1)$$

where $V_{i_{base}}$ is the voltage at bus i of the base network and $V_{i_{after}}$ is the voltage at bus i considering the load growth. A annual load growth of 1.4% [30] for a planning period of five years is considered in this study. The bus voltages during the

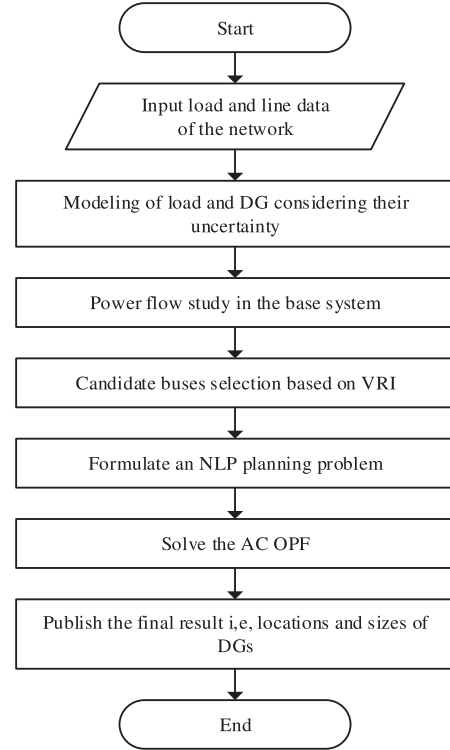


Fig. 2. The flowchart of the proposed optimal DG placement method.

planning period are calculated as follows:

$$V_{i_{after}} = V_{i_{base}} (1 + x\%)^y \quad (2)$$

where $x\%$ is the annual load growth and y is the planning period in years.

C. Power Flow Analysis

The power flow analysis is performed by formulating a non-linear AC OPF model such that all operational constraints (voltage limits, load variations, uncertainties in PV power generation) are satisfied for optimal DG placement in a distribution network.

D. Planning Problem Formulation

In this study, the planning is formulated as non-linear programming problem for optimal placement of DGs in distribution networks. The objective function is to minimize the total annual energy losses and improve the voltage profile. The details of the problem formulation is discussed in Section IV.

III. MODELING OF LOAD, DGs AND THEIR UNCERTAINTIES

Modeling components of a distribution network, such as load and DGs, is an essential aspect of microgrid planning.

A. Modeling of Load

The load profile is assumed to follow the IEEE-RTS [27] system's load model. This system provides the hourly peak load data as a percentage of the daily peak load over one year

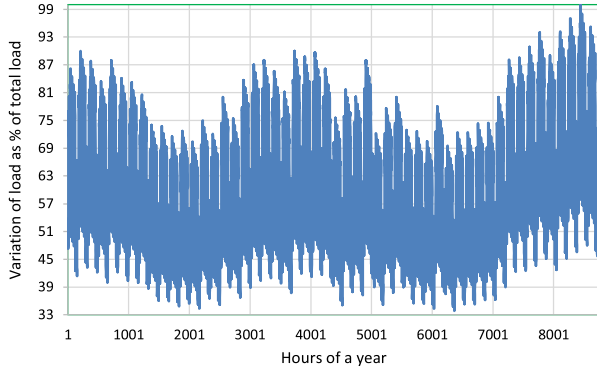


Fig. 3. Hourly load variation pattern of the IEEE-RTS system over one year.

considering seasonal variations in the load pattern. Fig. 3 shows the hourly load variation pattern of the IEEE-RTS system over one year.

B. Modeling of DGs

In this planning study, both dispatchable DGs (biomass power generation units) and non-dispatchable DGs (PV units) are optimally placed in a distribution network to minimize energy losses and satisfy operational constraints of the network. Modeling of these DGs is discussed below.

1) *Modeling of Biomass Power Generation Units*: The biomass power generation unit is modeled as dispatchable, i.e., its output is constant at the rated power without uncertainties. Therefore, the biomass unit can be selected based on its rated capacity.

2) *Modeling of PV Units*: The PV unit is modeled as non-dispatchable. The output power of PV units depends on many factors including PV modules' characteristics, the amount of solar irradiance, and the ambient temperature. Its output power is calculated by

$$T_{Cell} = T_A + s * \left(\frac{NOCT - 20}{0.8} \right) \quad (3)$$

$$I = s [I_{SC} + K_i (T_C - 25)] \quad (4)$$

$$V = V_{OC} - (K_v * T_C) \quad (5)$$

$$FF = \frac{V_{MPP} * I_{MPP}}{V_{OC} * I_{SC}} \quad (6)$$

$$P_{PV}(s) = N * FF * V * I \quad (7)$$

$$P_{PV}(s) = \frac{P_{STC} * s * [1 + K_p (T_C - 25)]}{S_{STC}} \quad (8)$$

where T_{Cell} , T_A , and $NOCT$ are the cell, ambient, and nominal operating temperature, respectively; P_{STC} , and S_{STC} are the power and solar irradiation at standard test conditions (STC), respectively; I_{SC} and V_{OC} are the short circuit current and open circuit voltage, respectively; K_i , K_v , and K_p are the temperature coefficient of the current, voltage, and power, respectively; FF is the fill factor; V_{MPP} and I_{MPP} are the voltage and current

at the maximum power point (MPP), respectively; and $P_{PV}(s)$ is the PV power generation for the irradiance, s .

C. Probabilistic Model of Uncertainty

Modeling uncertainties associated with variations of load and renewables in a distribution network is essential to integrate renewable DGs effectively in a planning study. Uncertainties are modeled in this study using the probability density function (PDF) discussed below.

1) *Uncertainty Model of Load*: The uncertainty in load variations is modeled using one year load data by a normal PDF [24].

$$f(P_l) = \frac{1}{\sigma_P \sqrt{2\pi}} \exp \left(-\frac{(P_l - \mu_P)^2}{2\sigma_P^2} \right) \quad (9)$$

$$f(Q_l) = \frac{1}{\sigma_Q \sqrt{2\pi}} \exp \left(-\frac{(Q_l - \mu_Q)^2}{2\sigma_Q^2} \right) \quad (10)$$

where $f(P_l)$ and $f(Q_l)$ are normal PDFs, μ_P and μ_Q are means of the normal distribution, σ_P and σ_Q are standard deviations of the normal distribution for active and reactive load, respectively.

2) *Uncertainty Model of PV Units*: The uncertain nature of solar irradiance makes the output power of PV units uncertain, which needs to be modeled properly to integrate PV units effectively in a planning study. The uncertainty of solar radiation is modeled by analyzing one-year solar irradiance data downloaded from the POWER Data Access Viewer (<https://power.larc.nasa.gov/data-access-viewer/>), and then, the beta PDF [3] can be determined by

$$f(s) = \frac{(\alpha + \beta)}{(\alpha) + (\beta)} * s^{(\alpha-1)} * (1-s)^{(\beta-1)} \quad (11)$$

$$0 \leq s \leq 1, \alpha \geq 0, \beta \geq 0 \quad (12)$$

$$\alpha = \frac{\mu * \beta}{1 - \mu}, \beta = (1 - \mu) * \left(\frac{\mu * (1 + \mu)}{\sigma^2} - 1 \right) \quad (13)$$

where $f(s)$ is the beta PDF of the solar irradiance; s is the solar irradiation in $\frac{kW}{m^2}$; α and β are shape parameters of the beta distribution; μ and σ are the mean and standard deviation of historical data, respectively.

3) *Combined Load-Solar Model*: To incorporate the load variation and the output power of PV units as multi-state variables in the planning problem formulation, the continuous PDFs of load and solar irradiance have been divided into several states [31]. In each state, the load and solar irradiance are within specific limits. The number of states is carefully selected for both normal and beta PDFs because a large number of states increases the computational burden, while a small number of states may affect the result accuracy. In this study, nine states for load and ten states for solar irradiance have been considered. The probability of each load and solar irradiance state can be calculated as follows:

$$\gamma(L_t) = \int_{l_1}^{l_2} f(l) dl \quad (14)$$

TABLE I
TECHNICAL SPECIFICATION OF FOUR SOLAR PV MODULES

Model	Maxeon 6	HiKu6 Mono PERC	NeONR	EverVolt
Manufacturer	Sun Power	Canadian Solar	LG	Panasonic
Efficiency (%)	22.8	21.5	22	21.2
NOCT (C)	--	41	44	44
Short Circuit Current (A)	--	14.17	10.84	10.55
Open Circuit Voltage (V)	--	37.6	42.9	44.1
Maximum Power (W)	440	420	380	370
MPP Voltage (V)	--	31.6	37.4	37.4
MPP Current (A)	--	13.31	10.17	9.9
Fill Factor	--	0.789	0.817	0.795
Current Temperature Coefficient	--	0.05	0.037	0.04
Voltage Temperature Coefficient	--	-0.26	-0.24	-0.24
Power Temperature Coefficient	-0.29	-0.34	-0.3	-0.26

$$\gamma(S_t) = \int_{s_1}^{s_2} f(s) ds \quad (15)$$

where $\gamma(L_t)$, and $\gamma(S_t)$ are the probability of the load and solar irradiance at the state t , respectively; l_2 , l_1 and s_2 , s_1 are the upper and lower limits of the load and solar irradiance at the state t , respectively.

A combined load-solar model is generated consisting of (9 load states \times 10 solar irradiance states) = total 90 states, assuming that the load and solar irradiance states are independent. Based on this assumption, the probability of any combination of load and solar irradiance state is obtained by convolving the two probabilities, as given in (16).

$$\gamma(C_t) = \gamma(L_t) \times \gamma(S_t) \quad (16)$$

where $\gamma(C_t)$ is the probability of the combined load-solar model at state t .

D. Selection of PV Units

Different types of PV panels with specific characteristics and specifications are available in the market. It is important to evaluate their performances before installing them in large scale into the system. Therefore, A brief study to select PV units demonstrated below based on the uncertainty model of solar irradiance is adopted in this paper. Four different PV panels are considered in Table I, and one of them will be chosen in this study in term of their capacity factor (CF).

A beta PDF for each time segment is generated using the hourly solar irradiance data for the site under study, and the CF for each PV module can be calculated as follows [32]:

$$\text{Capacity Factor} = \frac{P_{\text{average}}}{P_{\text{rated}}} \quad (17)$$

$$P_{\text{average}} = \sum_t P_t \times \gamma(S_t) \quad (18)$$

where P_{average} and P_{rated} are the average power generated and the rated power of the PV module, respectively; P_t is the output power at state t ; S_t is the solar insolation at state t ; $\gamma(S_t)$ is the probability of solar insolation at state t ; and T is the total number of solar insolation states. As shown in Fig. 4, among

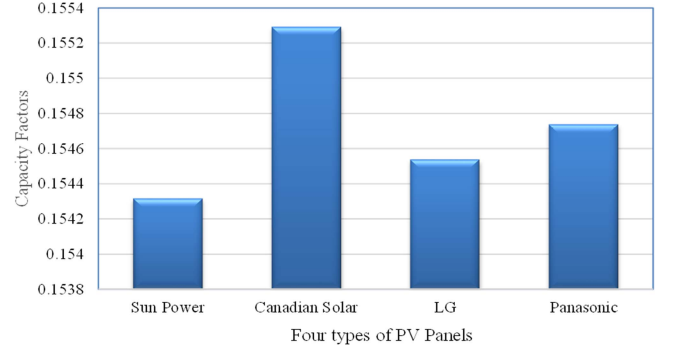


Fig. 4. The capacity factor of four types of PV panels.

the four types of PV modules, the HiKu6 Mono PERC module manufactured by Canadian Solar has the highest CF (0.1553), and thus, is chosen in this study.

IV. MATHEMATICAL FORMULATION

A. Assumptions

The following assumptions are made to implement the proposed DG placement method:

- 1) The system under study is in grid-connected mode, so the total DG integration is limited below the total demand of the network.
- 2) PV units are adopted as non-dispatchable DGs.
- 3) The biomass power generation unit is modeled as the dispatchable DG, and assumed to operate with a power factor of 0.95 [26], [19] as per the interconnection guideline of our local utility company, Saskatoon Light and Power [33].

B. Objective Functions

Different objectives have been selected for optimal DG placement in existing studies, such as minimizing costs, minimizing the total energy losses, minimizing emissions, maximizing profits, and improving reliability. However, one fundamental reason to implement microgrids in a distribution network is supplying load locally by DGs to minimize energy losses. Therefore, the optimal DG placement problem is formulated to minimize the total energy losses in this paper by

$$\min .OF = \sum_{t=1}^T P_{\text{Loss}_t} \times \gamma(C_t) \times 8760 \quad (19)$$

$$P_{\text{Loss}_t} = \sum_{\varphi} \sum_i^N \sum_j^N I_{i,j,t}^{\varphi 2} \times r_{ij} \quad (20)$$

where OF is the objective function to minimize the total annual energy losses, P_{Loss_t} is the total active power loss in p.u. in the network at state t ; T is the total number of states; N is the total number of nodes in the network; $I_{i,j,t}^{\varphi}$ is the current flow in p.u. between nodes i and j of phase φ at state t ; and r_{ij} is the resistance of a line between nodes i and j .

C. Constraints of the Problem

The constraints in this problem are explained below:

1) Voltage Limit:

$$V_{min} \leq v_{i,t}^\varphi \leq V_{max} \quad \forall i \neq 1 \quad (21)$$

where V_{min} and V_{max} are the minimum and maximum voltage limits, respectively; and $v_{i,t}^\varphi$ is the voltage in p.u. of node i of phase φ . In this paper, $V_{min} = 0.95$ p.u. and $V_{max} = 1.05$ p.u. are used for all buses of the network except the slack bus (bus 1). The slack bus has a constant voltage of 1 p.u. and a zero-degree phase angle.

2) DGs Capacity Limit:

$$S_{B_{min}} \leq S_{B_{i,t}}^\varphi \leq S_{B_{max}} \quad \forall i = m \quad (22)$$

$$P_{S_{min}} \leq P_{S_{i,t}}^\varphi \leq P_{S_{max}} \quad \forall i = m \quad (23)$$

where $S_{B_{min}}$ and $S_{B_{max}}$ are the minimum and maximum capacity of biomass power generation units, respectively; $S_{B_{i,t}}^\varphi$ is the capacity of the biomass generation unit at bus i ; $P_{S_{min}}$ and $P_{S_{max}}$ are the minimum and maximum capacity of PVs, respectively; P_{PV_i} is the capacity of PV unit at bus i ; and m is the total number of candidate buses.

3) *Power Factor Constraint*: The power factor is maintained constant at the point of interconnection of a biomass power generation unit by

$$P_{B_{i,t}}^\varphi = S_{B_{i,t}}^\varphi \times \cos \theta \quad (24)$$

$$Q_{B_{i,t}}^\varphi = S_{B_{i,t}}^\varphi \times \sin \theta \quad (25)$$

where $P_{B_{i,t}}^\varphi$ and $Q_{B_{i,t}}^\varphi$ are real and reactive power in p.u. of phase φ injected from the biomass power generation unit at node i and state t , respectively; $S_{B_{i,t}}^\varphi$ is the capacity of the biomass power generation unit of phase φ at node i and state t ; θ is the angle between the corresponding voltage and current.

4) Line Current Limit:

$$I_{i,j,t}^\varphi \leq I_{max} \quad \forall j = n \quad (26)$$

where $I_{i,j,t}^\varphi$ is the current flow in p.u. of phase φ between nodes i and j at state t ; I_{max} is the maximum limit of the current; and n is the total number of lines between buses.

5) Penetration Level of DGs:

$$\sum S_B = bm\% \text{ of demand} \quad (27)$$

$$\sum P_S = pv\% \text{ of demand} \quad (28)$$

where S_B is the capacity of the biomass power generation unit, and P_S is the capacity of the PV unit.

6) Generation-Demand Constraint:

$$\sum S_{load} \geq \sum S_{DG \text{ gen}} \quad (29)$$

where S_{load} is the load of the network, and $S_{DG \text{ gen}}$ is the generation capacity of DGs.

D. AC OPF

AC OPF analysis is used to solve the power flow problem in this study by satisfying operational constraints of the network and limitations of the problem formulation.

1) *Power Flow Equations*: Real and reactive power flow of phase φ in a three-phase distribution network between nodes i and j is calculated by

$$P_{i,j,t}^\varphi = \frac{v_{i,t}^{\varphi^2}}{z_{ij}^\varphi} \cos \theta_{ij}^\varphi - \frac{v_{i,t}^\varphi \times v_{j,t}^\varphi}{z_{ij}^\varphi} \cos (\delta_{i,t}^\varphi - \delta_{j,t}^\varphi + \theta_{ij}^\varphi) \quad (30)$$

$$Q_{i,j,t}^\varphi = \frac{v_{i,t}^{\varphi^2}}{z_{ij}^\varphi} \sin \theta_{ij}^\varphi - \frac{v_{i,t}^\varphi \times v_{j,t}^\varphi}{z_{ij}^\varphi} \sin (\delta_{i,t}^\varphi - \delta_{j,t}^\varphi + \theta_{ij}^\varphi) - \frac{b_{ij}^\varphi \times v_{i,t}^{\varphi^2}}{2} \quad (31)$$

where $P_{i,j,t}^\varphi$ and $Q_{i,j,t}^\varphi$ are real and reactive power in p.u. of phase φ between nodes i and j at state t ; z_{ij}^φ , θ_{ij}^φ , and b_{ij}^φ are the impedance in p.u., the angle of impedance, and the susceptance in p.u. of phase φ between nodes i and j ; $v_{i,t}^\varphi$, $\delta_{i,t}^\varphi$, and $v_{j,t}^\varphi$, $\delta_{j,t}^\varphi$ are the voltage in p.u., and the angle in radians of phase φ at nodes i and j , respectively.

2) *Power Balance Equations*: Real and reactive power are balanced at node i of the network by satisfying the following power balance equations:

$$P_{G_{i,t}}^\varphi + P_{B_{i,t}}^\varphi + P_{S_{i,t}}^\varphi \times (\%PV_t) - P_{L_{i,t}}^\varphi \times (\%L_t) = \sum_j P_{i,j,t}^\varphi \quad (32)$$

$$Q_{G_{i,t}}^\varphi + Q_{B_{i,t}}^\varphi - Q_{L_{i,t}}^\varphi \times (\%L_t) = \sum_j Q_{i,j,t}^\varphi \quad (33)$$

where $P_{G_{i,t}}^\varphi$ and $Q_{G_{i,t}}^\varphi$ are real and reactive power in p.u. of phase φ injected from the grid substation at node i and state t ; $P_{B_{i,t}}^\varphi$ and $Q_{B_{i,t}}^\varphi$ are real and reactive power in p.u. of phase φ injected from the biomass generation unit at node i and state t ; $P_{S_{i,t}}^\varphi$ is real power in p.u. of phase φ injected from a PV unit at node i and state t ; $P_{L_{i,t}}^\varphi$ and $Q_{L_{i,t}}^\varphi$ are real and reactive load in p.u. of phase φ connected to node i at state t ; $P_{i,j,t}^\varphi$ and $Q_{i,j,t}^\varphi$ are real and reactive power in p.u. of phase φ between nodes i and j at state t .

3) *Branch Current Equation*: The current flow in the branch between nodes i and j is calculated as follows:

$$I_{i,j,t}^\varphi = \frac{\sqrt{(P_{i,j,t}^\varphi)^2 + (Q_{i,j,t}^\varphi)^2}}{v_{i,t}^\varphi} \quad (34)$$

where $I_{i,j,t}^\varphi$ is the current flow in p.u. of phase φ between nodes i and j at state t ; $P_{i,j,t}^\varphi$ and $Q_{i,j,t}^\varphi$ are real and reactive power in p.u. of phase φ between nodes i and j at state t ; $v_{i,t}^\varphi$ is the voltage in p.u. of phase φ at node i .

4) Power Loss Equation:

$$P_{loss_t} = 0.5 \times \sum_\varphi \sum_i \sum_j \frac{(P_{i,j,t}^\varphi)^2 + (Q_{i,j,t}^\varphi)^2}{(v_{i,t}^\varphi)^2} \times r_{ij}^\varphi \quad (35)$$

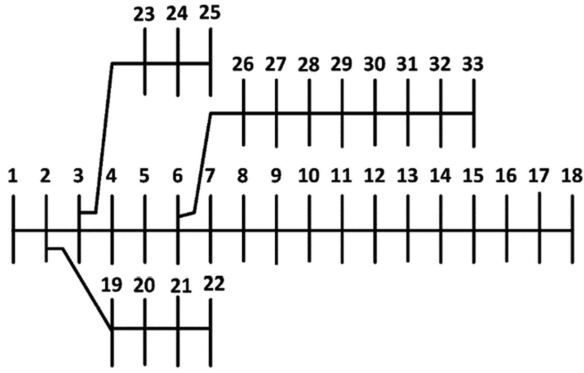


Fig. 5. IEEE 33-bus radial distribution test system (base case).

TABLE II
RESULTS OF OPTIMAL DG PLACEMENT IN IEEE 33-BUS TEST SYSTEM

Scenarios	Total Loss (MWh/year)	DG Locations (Bus Numbers)	Corresponding DG Sizes to bus No. (kVA or kW)
Without DGs	667.183	-	-
With DGs	213.654	BM:16,17,18,32,33 PV:17,32,33	247,191,93,249,243 11,186,161

where $P_{loss,t}$ is the total active power loss in p.u. in the network at state t ; $P_{i,j,t}^{\varphi}$ and $Q_{i,j,t}^{\varphi}$ are real and reactive power in p.u. of phase φ between nodes i and j at state t ; r_{ij}^{φ} is the resistance in p.u. of phase φ between nodes i and j ; $v_{i,t}^{\varphi}$ is the voltage in p.u. of phase φ at node i .

V. VALIDATION USING IEEE 33-BUS TEST SYSTEM

In this paper, IEEE 33-bus test system [5], [18] in Fig. 5 is used as the base case to validate the proposed method. In this base case, there are no DGs, and real and reactive power demand of the test system are 3.715 MW and 2.3 MVar, respectively. The base voltage and base MVA are 12.66 kV and 100 MVA, respectively. The total annual energy loss in the base case is 667.183 MWh, and the minimum nominal bus voltage is 0.9477 p.u. The simulation is carried out in GAMS using the CONOPT solver on a laptop computer with Intel i7, 2.6 GHz, and 16 GB RAM.

A. Results and Discussions

Biomass (BM) power generation and PV units are optimally placed in the IEEE 33-bus test system using the proposed method. The main objective is to minimize the total annual energy loss of the system and improve the bus voltage profile. The results for two scenarios, “Without DGs” and “With DGs”, are tabulated in Table II. The average voltage profile of the network for all 90 states is shown in Fig. 6.

Table II shows that the total annual energy loss is reduced from 667.183 MWh to 213.654 MWh by integrating 1023 kVA biomass generation (74.08% of the total DGs) and 358 kW PVs (25.92% of the total DGs). The total annual energy loss is reduced 67.98% by integrating 31.61% DGs of the total

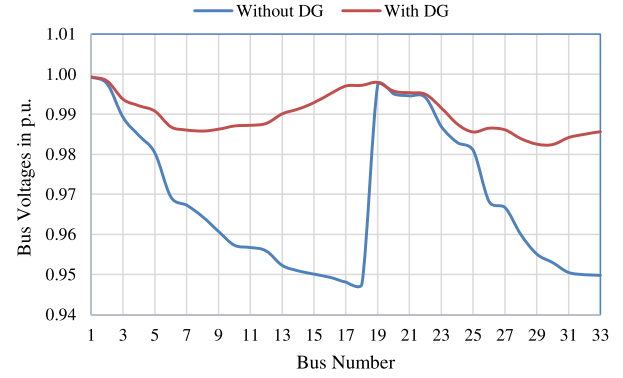
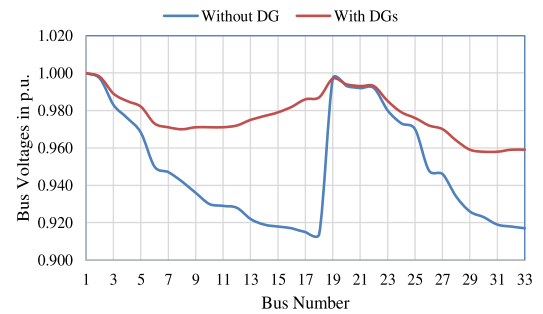
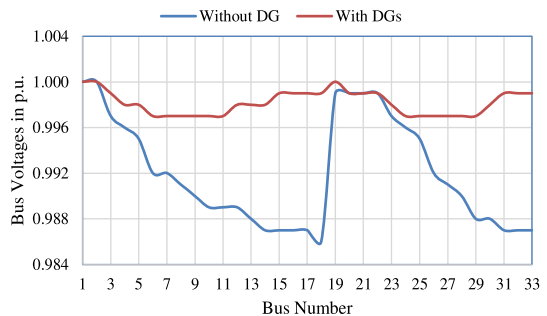


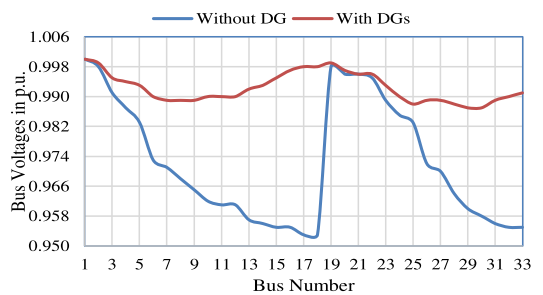
Fig. 6. The average bus voltage profile of IEEE 33-bus test system for all 90 states.



(a) Extreme State 1



(b) Extreme State 2



(c) A Typical State

Fig. 7. The bus voltage profile of IEEE 33-bus test system for three states.

demand of the network, and the voltage profile in Fig. 6 is also considerably improved.

Among 90 states considered, two extreme states and a typical state based on variations of load and PVs are demonstrated to observe their voltage profiles:

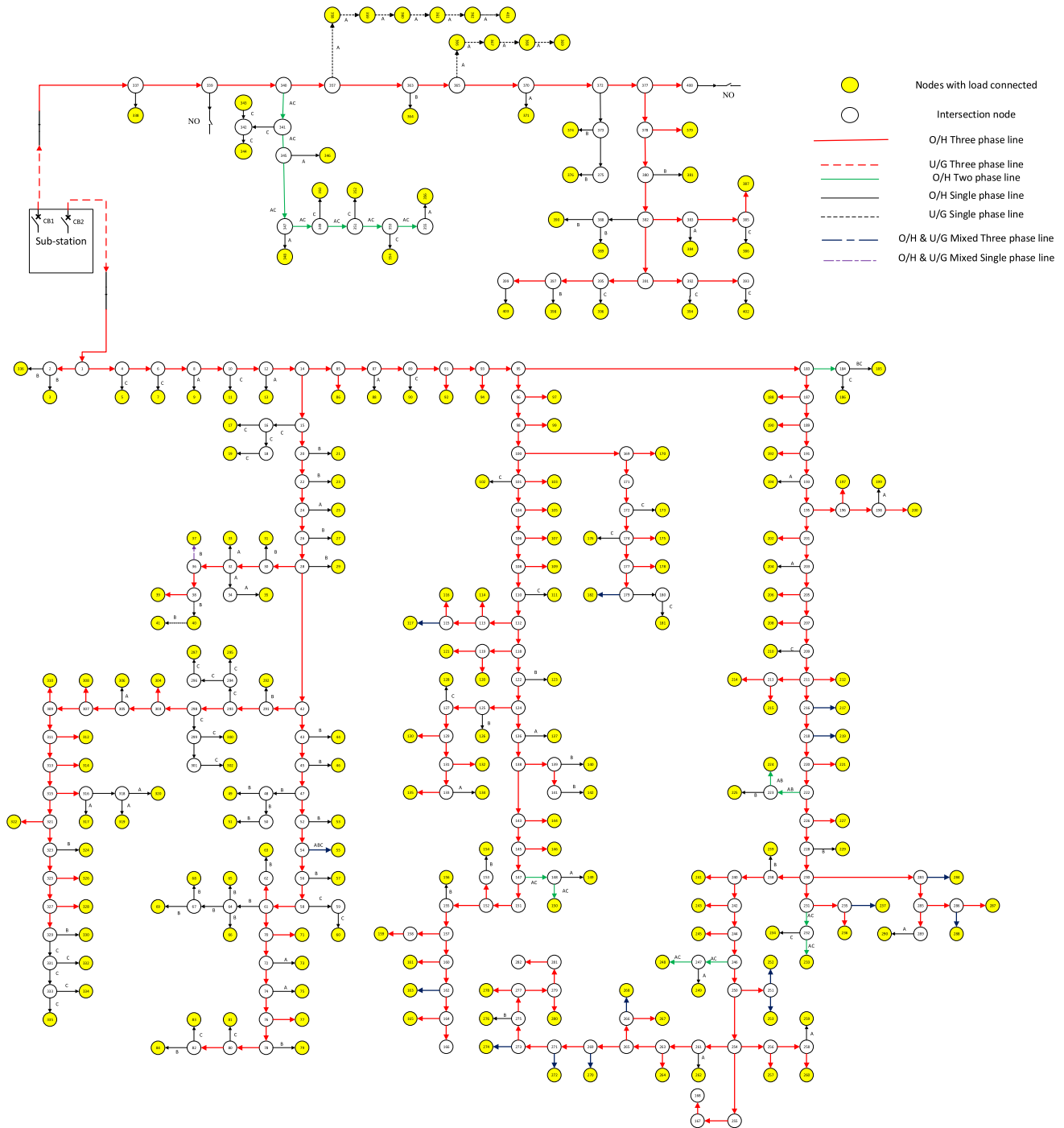


Fig. 8. Electrical single line diagram of one substation of the distribution system operated by Saskatoon Light and Power in Saskatoon, Canada.

- 1) *Extreme State 1*: PV power generation is 5.42% of the installed PV capacity, and load is 99% of the total load of the system.
- 2) *Extreme State 2*: PV power generation is 87.81% of the installed PV capacity, and load is 16.59% of the total load of the system.
- 3) *A Typical State*: PV power generation is 62.54% of the installed PV capacity, and load is 55.9% of the total load of the system.

Fig. 7(a) shows the voltage profile of the system in Extreme state 1. Before DG placement, voltages of some buses are below 0.95 p.u. due to a higher loading; after DG placement, all bus voltages are within the specified limits. Fig. 7(b) shows the voltage profile of the system in Extreme state 2, and voltages of all buses are within the limits before and after DG placement due to a lower loading. Fig. 7(c) shows the voltage profile of the system in a typical state, voltages are considerably improved

TABLE III
RESULTS OF OPTIMAL DG PLACEMENT IN IEEE 33-BUS TEST SYSTEM

Comparisons	Proposed Method	PSO in [5]	GA in [5]	TS in [27]	GSO in [6]	AGSO in [6]
Installed DGs as % of load	31.61	122.2	122.65	28.27	28.27	25.64
% Reduction of energy losses	67.98	72.3	79.6	38.73	38.77	38.91

after DG placement although all bus voltages are still within the limits before DG placement.

Our study indicates that the voltage profile of the network during all other states can be maintained within the permissible limits by optimally placing DGs in the test system.

B. Comparison of the Proposed and Existing Methods

To validate effectiveness of the proposed method, the results using the proposed method in IEEE 33-bus test system are compared with that using several existing methods in [5], [6], [27]. The optimal DG placement problem in IEEE 33-bus test system is solved using GA and PSO in [5]; using Tabu Search (TS) in [27]; and using Group Search Optimization (GSO) and Adaptive Group Search Optimization (AGSO) in [6]. The comparison in Table III validates the effectiveness of the proposed method. The proposed method only requires a smaller DG capacity to achieve a larger energy loss reduction compared to the five existing methods. These results also support the fact that the mathematical programming can find a global solution better than the metaheuristics.

VI. VALIDATION USING A REAL DISTRIBUTION SYSTEM

A. Real Distribution System of Local Utility

The proposed method is validated using a real 404-bus distribution system as shown in Fig. 8, which is one substation of a large distribution network operated by Saskatoon Light and Power in Saskatoon, Canada. The model is developed by utilizing existing lines and load data of two distribution feeders within the substation. Based on the given operation data, the network appears to be unbalanced among three phases.

In the base case of this modeled system, there are no DGs. The two feeders are energized from the 25/14.4 kV, 33.3 MVA grid substation. The real and reactive power demand of the base case are 12.288 MW (3.987, 4.345, and 3.956 MW on phases a, b, and c, respectively) and 5.951 MVar (1.931, 2.104, and 1.916 MVar on phases a, b, and c, respectively), assuming 70% loading of distribution transformers and 90% power factor.

If considering 1.14% annual load growth over a planning period of five years, the real and reactive power demand becomes 13.172 MW (4.274, 4.657, and 4.241 MW on phases a, b, and c, respectively) and 6.380 MVar (2.070, 2.256, and 2.054 MVar on phases a, b, and c, respectively).

The base voltage and base MVA are 14.4 kV and 100 MVA, respectively. The total annual energy losses obtained in the base case is 1246.02 MWh, and the minimum bus voltages are 0.974 p.u., 0.971 p.u., and 0.974 p.u. at phases a, b, and c of the

TABLE IV
RESULTS OF OPTIMAL DG PLACEMENT IN THE REAL DISTRIBUTION SYSTEM

Scenarios	Total Loss (MWh/year)	DG Locations (Bus Numbers)	Corresponding DG Sizes to bus No. (kVA or kW)
Without DGs	1246.02	-	-
With DGs	532.13	BM: 95, 124, 230, 254, 271, 327	600, 600, 600, 300, 300, 300 kVA
		PV: 14, 28, 42, 58, 78, 95, 124, 162, 230, 254, 271, 327, 357, 377, 391	195, 195, 195, 196, 196, 195, 195, 195, 195, 199, 200, 200 kW

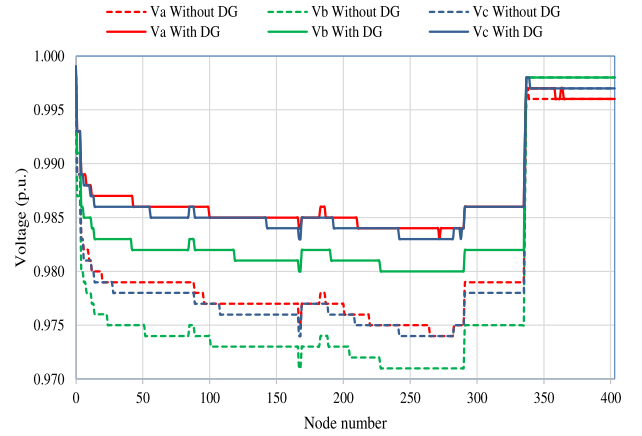


Fig. 9. The average bus voltage profile of the real distribution system for all 90 states.

unbalanced distribution system, respectively. The simulation is carried out in GAMS using the CONOPT solver.

B. Results and Discussions

Biomass (BM) power generation and PV units are optimally placed in this system using the proposed method to minimize the total annual energy losses and improve the bus voltage profile. The results of two scenarios, “Without DGs” and “With DGs”, are tabulated in Table IV. The average voltage profile of the system for all 90 states is shown in Fig. 9.

Table IV indicates that the total annual energy losses is reduced from 1246.02 MWh to 532.13 MWh by integrating 2700 kVA biomass power generation (47.86% of total DGs) and 2941 kW PV power generation (52.14% of total DGs) into the system. That means the total annual energy losses is reduced by 57.29% by integrating 38.54% DGs of total demand of the system. The voltage profile in Fig. 9 is also considerably improved along with the energy loss reduction. After integrating DGs, the minimum bus voltages are 0.983 p.u., 0.980 p.u., and 0.983 p.u. at phases a, b, and c, respectively.

Two extreme states and a typical state defined in Section V based on variations of load and PV power generation are also analyzed in this large real system to observe the voltage profiles in these states. Fig. 10(a) shows the voltage profile of the system in Extreme state 1, and the bus voltages of all phases are maintained above 0.95 p.u. before and after DG placement. Fig. 10(b)

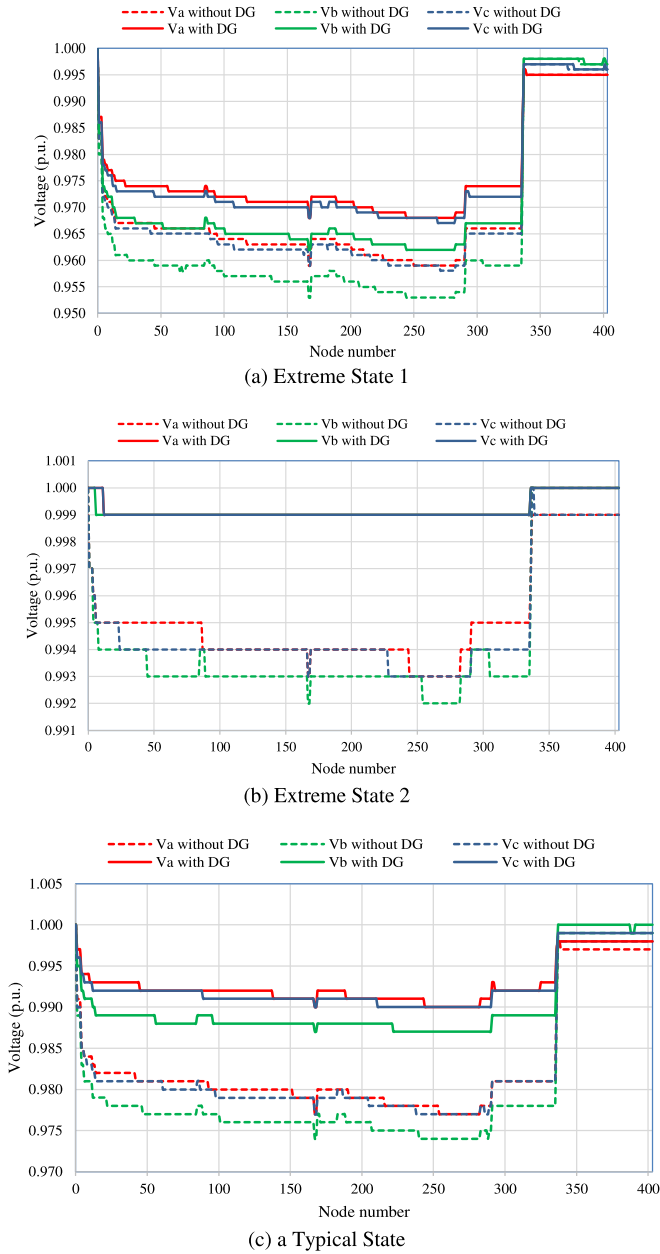


Fig. 10. The bus voltage profile of the real distribution system for three states.

shows the voltage profile of the system in Extreme state 2, and the voltages of all buses are within the specified limits before and after DG placement. Fig. 10(c) shows the voltage profile of the system in a typical state, and the voltages of all buses are considerably improved and maintained within the specified limits due to optimal placement of DGs. Based on our study, the voltage profiles of all other states are also maintained within the permissible limits.

VII. CONCLUSION

In this paper, an effective method is proposed to allocate DGs optimally in microgrid planning by defining a new index, Voltage Regulation Index, to select candidate locations for DG

placement in distribution networks. The objective is formulated to minimize the total annual energy losses of the system subject to certain operational constraints considering uncertainties associated with load variations and renewable energy sources. Non-linear programming and AC optimal power flow are used to obtain optimal solutions of this planning problem.

Case studies for an IEEE 33-bus test system and a 404-bus real distribution system using the proposed method are demonstrated, where dispatchable and non-dispatchable DGs are optimally placed, and the voltage profile of the system can be maintained within the permissible limits under various system operating conditions. The proposed method is proven to be effective by comparing with several existing methods in the literature.

REFERENCES

- [1] S. M., R. H. Shawon, X. Liang, and M. Janbakhsh, "Microgrid planning in distribution networks considering optimal placement of distributed generation units," in *Proc. IEEE Ind. Appl. Soc. Annu. Meeting*, 2022, pp. 1–8.
- [2] M. H. S. Boloukat and A. A. Foroud, "Multiperiod planning of distribution networks under competitive electricity market with penetration of several microgrids, part I: Modeling and solution methodology," *IEEE Trans. Ind. Inform.*, vol. 14, no. 11, pp. 4884–4894, Nov. 2018, doi: [10.1109/TII.2018.2807396](https://doi.org/10.1109/TII.2018.2807396).
- [3] S. A. Arefifar, Y. A.-R. I. Mohamed, and T. H. M. EL-Fouly, "Optimum microgrid design for enhancing reliability and supply-security," *IEEE Trans. Smart Grid*, vol. 4, no. 3, pp. 1567–1575, Sep. 2013, doi: [10.1109/TSG.2013.2259854](https://doi.org/10.1109/TSG.2013.2259854).
- [4] *IEEE Guide for Design, Operation, and Integration of Distributed Resource Island Systems with Electric Power Systems*, IEEE Standard 1547.4-2011, Jul. 2011, doi: [10.1109/IEEESTD.2011.5960751](https://doi.org/10.1109/IEEESTD.2011.5960751).
- [5] M. V. Kirthiga, S. A. Daniel, and S. Guranathan, "A methodology for transforming an existing distribution network into a sustainable autonomous micro-grid," *IEEE Trans. Sustain. Energy*, vol. 4, no. 1, pp. 31–41, Jan. 2013, doi: [10.1109/TSTE.2012.2196771](https://doi.org/10.1109/TSTE.2012.2196771).
- [6] N. Daryani, K. Zare, and S. Tohidi, "Design for independent and self-adequate microgrids in distribution systems considering optimal allocation of DG units," *IET Gener. Transm. Distrib.*, vol. 14, no. 5, pp. 728–734, Mar. 2020, doi: [10.1049/iet-gtd.2019.0379](https://doi.org/10.1049/iet-gtd.2019.0379).
- [7] S. A. Arefifar and Y. A.-R. I. Mohamed, "DG mix, reactive sources and energy storage units for optimizing microgrid reliability and supply security," *IEEE Trans. Smart Grid*, vol. 5, no. 4, pp. 1835–1844, Jul. 2014, doi: [10.1109/TSG.2014.2307919](https://doi.org/10.1109/TSG.2014.2307919).
- [8] W. Yuan, J. Wang, F. Qiu, C. Chen, C. Kang, and B. Zeng, "Robust optimization-based resilient distribution network planning against natural disasters," *IEEE Trans. Smart Grid*, vol. 7, no. 6, pp. 2817–2826, Nov. 2016, doi: [10.1109/TSG.2015.2513048](https://doi.org/10.1109/TSG.2015.2513048).
- [9] A. Andreotti, G. Carpinelli, F. Mottola, D. Proto, and A. Russo, "Decision theory criteria for the planning of distributed energy storage systems in the presence of uncertainties," *IEEE Access*, vol. 6, pp. 62136–62151, 2018, doi: [10.1109/ACCESS.2018.2876236](https://doi.org/10.1109/ACCESS.2018.2876236).
- [10] A. O. Rousis, I. Konstantelos, and G. Strbac, "A planning model for a hybrid AC–DC microgrid using a novel GA/AC OPF algorithm," *IEEE Trans. Power Syst.*, vol. 35, no. 1, pp. 227–237, Jan. 2020, doi: [10.1109/TPWRS.2019.2924137](https://doi.org/10.1109/TPWRS.2019.2924137).
- [11] S. Mohamed, M. F. Shaaban, M. Ismail, E. Serpedin, and K. A. Qaraqe, "An efficient planning algorithm for hybrid remote microgrids," *IEEE Trans. Sustain. Energy*, vol. 10, no. 1, pp. 257–267, Jan. 2019, doi: [10.1109/TSTE.2018.2832443](https://doi.org/10.1109/TSTE.2018.2832443).
- [12] A. A. Hamad, M. E. Nassar, E. F. El-Saadany, and M. M. A. Salama, "Optimal configuration of isolated hybrid AC/DC microgrids," *IEEE Trans. Smart Grid*, vol. 10, no. 3, pp. 2789–2798, May 2019, doi: [10.1109/TSG.2018.2810310](https://doi.org/10.1109/TSG.2018.2810310).
- [13] A. H. Yazdavar, M. F. Shaaban, E. F. El-Saadany, M. M. A. Salama, and H. H. Zeineldin, "Optimal planning of distributed generators and shunt capacitors in isolated microgrids with nonlinear loads," *IEEE Trans. Sustain. Energy*, vol. 11, no. 4, pp. 2732–2744, Oct. 2020, doi: [10.1109/TSTE.2020.2973086](https://doi.org/10.1109/TSTE.2020.2973086).

- [14] F. S. Gazijahani and J. Salehi, "Robust design of microgrids with reconfigurable topology under severe uncertainty," *IEEE Trans. Sustain. Energy*, vol. 9, no. 2, pp. 559–569, Apr. 2018, doi: [10.1109/TSST.2017.2748882](#).
- [15] M. Kumar and B. Tyagi, "An optimal multivariable constrained nonlinear (MVCNL) stochastic microgrid planning and operation problem with renewable penetration," *IEEE Syst. J.*, vol. 14, no. 3, pp. 4143–4154, Sep. 2020, doi: [10.1109/JSYST.2019.2963729](#).
- [16] A. Mohsenzadeh, C. Pang, and M.-R. Haghifam, "Determining optimal forming of flexible microgrids in the presence of demand response in smart distribution systems," *IEEE Syst. J.*, vol. 12, no. 4, pp. 3315–3323, Dec. 2018, doi: [10.1109/JSYST.2017.2739640](#).
- [17] A. Khodaei, S. Bahramirad, and M. Shahidehpour, "Microgrid planning under uncertainty," *IEEE Trans. Power Syst.*, vol. 30, no. 5, pp. 2417–2425, Sep. 2015, doi: [10.1109/TPWRS.2014.2361094](#).
- [18] N. Kanwar, N. Gupta, K. R. Niazi, and A. Swarnkar, "Optimal distributed resource planning for microgrids under uncertain environment," *IET Renew. Power Gener.*, vol. 12, no. 2, pp. 244–251, Feb. 2018, doi: [10.1049/iet-rpg.2017.0085](#).
- [19] S. F. Contreras, C. A. Cortes, and J. M. A. Myrzik, "Optimal microgrid planning for enhancing ancillary service provision," *J. Mod. Power Syst. Clean Energy*, vol. 7, no. 4, pp. 862–875, Jul. 2019, doi: [10.1007/s40565-019-0528-3](#).
- [20] K. Karimizadeh, S. Soleymani, and F. Faghihi, "Optimal placement of DG units for the enhancement of MG networks performance using coalition game theory," *IET Gener. Transmiss. Distrib.*, vol. 14, no. 5, pp. 853–862, Mar. 2020, doi: [10.1049/iet-gtd.2019.0070](#).
- [21] M. Khalid, U. Akram, and S. Shafiq, "Optimal planning of multiple distributed generating units and storage in active distribution networks," *IEEE Access*, vol. 6, pp. 55234–55244, 2018, doi: [10.1109/ACCESS.2018.2872788](#).
- [22] Z. Wang, B. Chen, J. Wang, J. Kim, and M. M. Begovic, "Robust optimization based optimal DG placement in microgrids," *IEEE Trans. Smart Grid*, vol. 5, no. 5, pp. 2173–2182, Sep. 2014, doi: [10.1109/TSG.2014.2321748](#).
- [23] F. Samadi Gazijahani and J. Salehi, "Optimal bilevel model for stochastic risk-based planning of microgrids under uncertainty," *IEEE Trans. Ind. Inform.*, vol. 14, no. 7, pp. 3054–3064, Jul. 2018, doi: [10.1109/TII.2017.2769656](#).
- [24] J. Mitra, M. R. Vallem, and C. Singh, "Optimal deployment of distributed generation using a reliability criterion," *IEEE Trans. Ind. Appl.*, vol. 52, no. 3, pp. 1989–1997, May/Jun. 2016, doi: [10.1109/TIA.2016.2517067](#).
- [25] S. A. Arefifar, Y. A.-R. I. Mohamed, and T. H. M. El-Fouly, "Comprehensive operational planning framework for self-healing control actions in smart distribution grids," *IEEE Trans. Power Syst.*, vol. 28, no. 4, pp. 4192–4200, Nov. 2013, doi: [10.1109/TPWRS.2013.2259852](#).
- [26] S. A. Arefifar and Y. A.-R. I. Mohamed, "Probabilistic optimal reactive power planning in distribution systems with renewable resources in grid-connected and islanded modes," *IEEE Trans. Ind. Electron.*, vol. 61, no. 11, pp. 5830–5839, Nov. 2014, doi: [10.1109/TIE.2014.2308144](#).
- [27] S. A. Arefifar, Y. A.-R. I. Mohamed, and T. H. M. El-Fouly, "Supply-Adequacy-Based optimal construction of microgrids in smart distribution systems," *IEEE Trans. Smart Grid*, vol. 3, no. 3, pp. 1491–1502, Sep. 2012, doi: [10.1109/TSG.2012.2198246](#).
- [28] L. Zhu, X. Zhou, X.-P. Zhang, Z. Yan, S. Guo, and L. Tang, "Integrated resources planning in microgrids considering interruptible loads and shiftable loads," *J. Mod. Power Syst. Clean Energy*, vol. 6, no. 4, pp. 802–815, Jul. 2018, doi: [10.1007/s40565-017-0357-1](#).
- [29] A. Selim, S. Kamel, A. S. Alghamdi, and F. Jurado, "Optimal placement of DGs in distribution system using an improved harris hawks optimizer based on Single- and Multi-Objective approaches," *IEEE Access*, vol. 8, pp. 52815–52829, 2020, doi: [10.1109/ACCESS.2020.2980245](#).
- [30] Saskatoon Light & Power, "Annual report attachment 1," p. 7, 2017.
- [31] Y. M. Atwa and E. El-Saadany, "Probabilistic approach for optimal allocation of wind-based distributed generation in distribution systems," *IET Renewable Power Gener.*, vol. 5, pp. 79–88, 2011, doi: [10.1049/iet-rpg.2009.0011](#).
- [32] Y. M. Atwa, E. F. El-Saadany, M. M. A. Salama, and R. Seethapathy, "Optimal renewable resources mix for distribution system energy loss minimization," *IEEE Trans. Power Syst.*, vol. 25, no. 1, pp. 360–370, Feb. 2010, doi: [10.1109/TPWRS.2009.2030276](#).
- [33] Saskatoon Light & Power, "Interconnection guideline, IG2007 rev. 0 for the connection of distributed generation to the Saskatoon light & power electrical distribution system," p. 18, May 2007.



Shah Mohammad Rezwatul Haque Shawon (Student Member, IEEE) was born in Gaibandha, Rangpur, Bangladesh. He received the B.Sc. degree in electrical and electronic engineering from the Rajshahi University of Engineering and Technology, Rajshahi, Bangladesh, in 2013. He is currently working toward the M.Sc. degree in electrical engineering with the University of Saskatchewan, Saskatoon, SK, Canada. From 2014 to 2015, he was a Lecturer with Prime University, Dhaka, Bangladesh, and the Green University of Bangladesh, Dhaka. In June, 2015, he joined Dhaka Power Distribution Company Limited (An Enterprise of the Government of the People's Republic of Bangladesh) as an Assistant Engineer. His research interests include power systems, renewable energy, and microgrids. He is a Member of the Institution of Engineers, Bangladesh.



Xiaodong Liang (Senior Member, IEEE) was born in Lingyuan, Liaoning, China. She received the B.Eng. and M.Eng. degrees in electrical engineering from Shenyang Polytechnic University, Shenyang, China, in 1992 and 1995, respectively, the M.Sc. degree in electrical engineering from the University of Saskatchewan, Saskatoon, SK, Canada, in 2004, and the Ph.D. degree in electrical engineering from the University of Alberta, Edmonton, AB, Canada, in 2013. From 1995 to 1999, she was a Lecturer with Northeastern University, Shenyang, China. In October

2001, she joined Schlumberger in Edmonton, Canada, and was promoted to a Principal Power Systems Engineer with this world's leading oil field service company in 2009. After serving Schlumberger for almost 12 years, from 2013 to 2019, she was with Washington State University, Vancouver, WA, USA, and Memorial University of Newfoundland, St. John's, NL, Canada, as an Assistant Professor and later an Associate Professor. In July 2019, she joined the University of Saskatchewan, Saskatoon, SK, Canada, where she is currently an Associate Professor and Canada Research Chair of Technology Solutions for Energy Security in Remote, Northern, and Indigenous Communities. From 2019 to 2022, she was an Adjunct Professor with the Memorial University of Newfoundland. Her research interests include power systems, renewable energy, and electric machines. Dr. Liang is a registered Professional Engineer in the province of Saskatchewan, Canada, a Fellow of IET, and a Deputy Editor-in-Chief of IEEE TRANSACTIONS ON INDUSTRY APPLICATIONS.



Mehrnoosh Janbakhsh (Senior Member, IEEE) received the Bachelor's of Science degree in electrical engineering from the K. N. Toosi University of Technology, Tehran, Iran, in 1997, and the Master's of Engineering degree in electrical engineering from the University of Saskatchewan, Saskatoon, SK, Canada, in 2011. She is currently a Senior Engineer with Distribution Engineering, BC Hydro, Burnaby, BC, Canada. Before that, she was a Smart Grid Senior Project Management Engineer with Saskatoon Light and Power, Saskatoon, SK, Canada. She has about

20 years of experience in telecommunications and power engineering. She led the power distribution and transmission team in Saskatoon Light and Power for eight years, and her team was responsible for overhead and underground designs, customer connects, updating the material specifications, construction standards and operations. Several year ago, she became the group leader of the Smart Grid group within Saskatoon Light and Power, and her team was responsible for communications, cyber security, IT, protection and control, and smart grid. She is a Volunteer Assessor with APEGS and also a Volunteer with the IEEE Smart City Group.